

SAGE: Stealthy Attack GEneration for Cyber-Physical Systems

Michael Biehler, Zhen Zhong, and Jianjun Shi

Abstract—Cyber-physical systems (CPS) have been increasingly attacked by hackers. Recent studies have shown that CPS are especially vulnerable to insider attacks, in which case the attacker has full knowledge of the systems configuration. To better prevent such types of attacks, we need to understand how insider attacks are generated. Typically, there are three critical aspects for a successful insider attack: (i) Maximize damage, (ii) Avoid detection and (iii) Minimize the attack cost. In this paper we propose a “Stealthy Attack GEneration” (SAGE) framework by formulating a novel optimization problem considering these three objectives and the physical constraints of the CPS. By adding small worst-case perturbations to the system, the SAGE attack can generate significant damage, while remaining undetected by the systems monitoring algorithms. The proposed methodology is evaluated on several anomaly detection algorithms. The results show that SAGE attacks can cause severe damage while staying undetected and keeping the cost of an attack low. Our method can be accessed in the supplementary material of this paper to aid researcher and practitioners in the design and development of resilient CPS and detection algorithms.

Index Terms—Attack Generation, Cyber-Physical Systems (CPS), Network-level security and protection



1 INTRODUCTION

Cyber-physical systems (CPS) have been increasingly attacked by hackers [1]. The system integrity and security of CPS is of major importance, since any successful attack can lead to severe economic loss, equipment damage, or even loss of human life [2]. Understanding insider attacks is of great importance since they are becoming more frequent and more resources are needed to detect them [3, 4]. An average time of 77 days to detect an insider attack [3] indicates that the level of sophistication of attackers is increasing and detection algorithms need to consider the complex structure of attacks executed by hackers who have full knowledge of the system.

Supervised machine learning techniques have achieved superior detection performance on existing types of attack generation schemes [5], [6], [7]. However, those type of supervised learning techniques require strong assumptions and can be considered as a best-case scenario for the defender of the system. In particular, historical training data needs to be available with labels of in control (e.g., no attack) and attack conditions. Additionally, the current attack needs to come from the same generative process as the historical attacks.

In an unsupervised setting, control charts are commonly used to detect cyber-attacks in CPS [8]. However, in the research reported in this paper, we discover that if an attacker knows the current configuration of a CPS, most

existing algorithms have vulnerabilities, which can be bypassed by the attackers. In a nutshell, the existing detection algorithms are based on very strong assumptions on the attack schemes, which may not mimic the behavior of an insider attacker. An effective detection algorithm requires the defenders to change perspective and “think like a hacker” to identify the weaknesses of a system and possible solutions to prevent intrusions.

Given the lack of comprehensive and rigorous methods to generate insider attacks in CPS, we propose a general and comprehensive framework for “Stealthy Attack GEneration” (SAGE) in CPS. By formalizing a novel optimization problem, the SAGE framework considers the three main objectives of an attacker: (i) Maximize damage, (ii) Avoid detection, and (iii) Minimize the attack cost. By applying small, intentional, worst-case perturbations to the system variables, the SAGE attack will lead to unexpected and dangerous misbehavior of the system, while remaining undetected.

To show the generality of our approach, we generate stealthy attacks and validate the SAGE framework on two case studies: an image anomaly detection and a hot rolling process simulated in MATLAB Simulink. In the image case study, SSD [9] and CNN-LIME are used as detection algorithms. In the case study of hot rolling process, seven commonly used detection algorithms are utilized, which include a Support Vector Machine (SVM), k Nearest Neighbor (kNN), Random Forest (RF), Bagging, Gradient Boosting Machine (GBM), Decision Tree (DT), and Deep Neural Network (DNN).

Our work contributes to the understanding of stealthy attacks in CPS. The results provide a case for the severe consequences of properly executed insider attacks. Furthermore, this research serves as a cornerstone for development of more effective detection algorithms and more

- M. Biehler is with the H. Milton Stewart School of Industrial and Systems Engineering, Georgia Tech, GA 30332 USA. E-mail: michael.biehler@gatech.edu.
- Z. Zhong is with the H. Milton Stewart School of Industrial and Systems Engineering, Georgia Tech, GA 30332 USA. E-mail: zhongzhen@gatech.edu.
- J. Shi is with the H. Milton Stewart School of Industrial and Systems Engineering, Georgia Tech, GA 30332. E-mail: jianjun.shi@isye.gatech.edu.

resilient and robust CPS design.

The remaining parts of this paper are organized as follows. In Section 2, we review related literature to highlight the necessity of this research. In Section 3, we present the mathematical description of a CPS, formulate the optimization problem, and propose the algorithm for solving this problem. In Section 4, the methods proposed in Section 3 are validated through case studies. Finally, Section 5 concludes the paper.

2 LITERATURE REVIEW

Due to the rise of smart manufacturing, CPS like power grids is increasingly exposed to cyber-attacks [10], [11], [12]. Attacks like the computer worm “Stuxnet” attacking Siemens industrial software in 2010 or the phishing attack on a German steel mill leading to severe equipment failures in 2014 are some of the most prominent examples for the vulnerability of CPS to cyber-attacks. Even though the field of information technology on cybersecurity is rapidly developing, the unique characteristics of CPS require specific attention [8]. CPSs have grown from stand-alone systems with little security protection to highly interconnected systems that can be easily targeted by attackers over the internet [13].

In general, the first step of an attacker is to gain knowledge of the system by identifying the network topology, software, critical targets, and monitoring schemes against cyber-attacks [14]. Then the first line of defense consisting of the firewall and an intrusion prevention system needs to be bypassed. After the attacker has full access to the CPS, the goal is to perturb the control systems and make as much damage as possible while staying undetected. The detection methods at the level of CPS like networks, systems and process data are considered the second line of defense.

In recent years, multiple detection algorithms have developed for the second line of defense [5], [15], [16], [17], [18], [19], [20]. These methods mainly employ data-driven supervised machine learning methods like neural networks to detect cyber-attacks in CPS and achieve very high detection performance. However, those methods do not focus on the design of secure and reliable CPS. Therefore, those types do not focus on the modeling of stealthy attacks as shown in Fig. 1. Additionally, these detection methods only work if the same type of attack is carried out again. Thus, the data generating process of any new attack needs to be the same, which is not reasonable in practice due to the vast number of attackers and methods in this field.

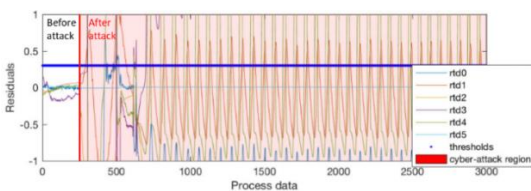


Fig. 1. An example of a non-stealthy attack on CPS [8]

Since companies usually do not publish data after they have been attacked, there is a fundamental need to generate attacks on CPS to study and evaluate their cybersecurity. However, in most of the existing literature, the attack scenarios are not very realistic and do not follow a comprehensive, rigorous, and holistic framework that considers the objectives of an attacker and the specific requirements of CPS. Previous research has introduced a framework to generate integrity attacks by formalizing the adversary's strategy as a constrained control problem [21]. However, this method is only applicable to CPS that can be modeled as discrete linear time-invariant systems equipped with a Kalman filter, Linear Quadratic Gaussian (LQG) controller, and χ^2 detector [21]. A constrained adversarial machine learning technique for CPS [22] has been proposed, but only considers the intrinsic constraints of the physical systems, which is only one of the objectives of an attacker and furthermore assumes that only a subset of sensors is compromised.

Some prior work has addressed the problem of generating adversarial examples for machine learning systems [23], [24], [25], [26], but not in the context of fooling monitoring schemes in CPS by making very small perturbations of the control variables. In a cyber-attack CPS problem, the goal is not solely to fool a machine learning classifier, but to make damage on the physical components by considering the system model, the physical constraints, multiple monitoring algorithms and the attack cost. The existing literature on generative models in the field of cyber security [27], [28], [29] mainly focuses on adversarial data, which could lead to wrong conclusions of a machine learning model. By utilizing the understanding of the generative model, more robust and reliable machine learning models can be developed. The SAGE can be viewed as a generalization of the adversarial data concept since loss functions and the results mentioned above can be integrated into SAGE formulation.

3 SAGE METHODOLOGY

This section first describes the system model used to model the dynamics of CPS. Afterwards, the SAGE framework is introduced, which considers the main objectives of an attacker consisting of maximizing the damage to the system while staying undetected and keeping the cost of an attack low.

3.1 System Modeling

The following section will describe the model used to characterize the system dynamics of CPS. For a general CPS, we will assume the following data scenario:

The process outputs $Y_{k,t}$ from each subsystem k at time t can include multiple functional curves of the same length, images, structured point clouds and categorical variables. Furthermore, we assume for each subsystem $i = 1, \dots, k$ there are $j = 1, \dots, q_i$ inputs at time t represented by $u_{ij,t}$. Contrary to an abundance of previous research in this field, we will assume that the effect of the inputs on the

outputs can have a nonlinear relationship. This allows more realistic modeling of complex CPS. This formulation can be adjusted appropriately according to the system model with the best fit to the historical data from a variety of potential models like linear regression, gaussian process model, or neural networks. Therefore, the system model can be represented as

$$Y_{k,t} = B_{k0} + \sum_{i=1}^k \sum_{j=1}^{q_i} g_{ij,t}(u_{ij,t}, \theta) + E_k \quad (1)$$

where $g_{ij,t}(u_{ij,t}, \theta)$ ($i = 1, \dots, k; j = 1, \dots, q_i$) are some nonlinear functions with the parameter vector θ , and E_k is a matrix containing the modeling error for each subsystem where every entry is a zero mean additive Gaussian noise with variance $\delta^2_{E,k}$. The offset matrices are denoted by B_{k0} .

3.2 Stealthy Attack GEneration (SAGE)

Since 68% of organizations in a recent survey indicated that they are moderately to extremely vulnerable to insider attacks [3], we assume the worst-case scenario, where the attacker has full control and knowledge of the system. In particular, the attacker knows the process model and can inject data at any point and time.

Therefore, we will define a problem that fulfills the following three main objectives of an attacker:

1. *Maximize Damage*: The goal of an attacker is to cause damage to physical components such as machines, equipment, parts, assemblies, and products in CPS. Thus, the cyber attacker can cause devastating damage to CPS by increasing the wear, breakage, scrap, or any other changes to the original design [20].
2. *Avoid Detection*: The aim of an attacker is to manipulate CPS in such a way that the altered control actions stay undetected. Most equipment has some hard-wired safety mode that will shut down the machines once they reach a safety relevant operating condition [30]. Therefore, staying undetected will directly contribute to the first objective to maximize damage. Once an intrusion is detected by the consecutive layers of cyber-attack detection, for example, on the firewall level, it would be hard to determine for the defender if and which parameters were actually changed by the intruder, which will cause even more downstream damage.
3. *Minimize Attack Cost*: Attacking all control actions and replaying old data for all of them might be costly or complicated because different sensing data are saved in different databases and operating systems and many resources would be needed. Therefore, the attacker will want to keep the cost of an attack low.

Consequently, the attacker's optimization problem is formulated as Eq. 2, which exploits CPS system model and the weaknesses of the detection algorithm while considers the physical constraints of the system.

$$\min_{\mathbf{u}_t^A} -\|Y_{k,t}^{ref} - B_{k0} + \sum_{i=1}^k \sum_{j=1}^{q_i} g_{ij,t}(u_{ij,t}^A, \theta)\|_p + \lambda_1 \|f(\mathbf{u}_t^{IC}) - f(\mathbf{u}_t^A)\|_p + \lambda_2 \|h(\mathbf{u}_t^A, \mathbf{u}_{t-1}^A)\|_p + \lambda_3 \mathcal{C}(\mathbf{u}_t^A) \quad (2)$$

where $Y_{k,t}^{ref}$ denotes the reference or desired process output of subsystem k at time t under normal conditions, and $\mathbf{u}_t^A = (u_{11,t}, u_{12,t}, \dots, u_{21,t}, \dots, u_{kq_i,t})$ are the perturbed process inputs of all k subsystems, and q_i variables by the attacker, which should close to the in-control process inputs $\mathbf{u}_t^{IC} = (u_{11,t}^{IC}, u_{12,t}^{IC}, \dots, u_{21,t}^{IC}, \dots, u_{kq_i,t}^{IC})$. The differences are denoted in terms of the ℓ_p -norm to allow for flexible modeling requirements. Here are further explanations of each term in Eq. 2:

- The first term incorporates the first objective of the attacker, which is to maximize the damage to the system. This is equivalent to minimizing the negative of difference between reference system response and the predicted output for all inputs $\mathbf{u}_{ij,t}^A$.
- The second term ensures that the attack does not get detected. Depending on the detection algorithm, we choose a mapping function $f(\cdot)$ so attacker's control actions are close to "in-control" actions.
- The third term ensures that the physical constraints of the CPS are met via a function $h(\cdot)$, that maps the attacker's actions to the physical constraints. Control actions can only change within physical limits e.g., the magnitude of change in consecutive time steps should be small.
- The last term keeps the cost of attack low by considering how costly it is to attack a particular control action.

The system model as introduced in Section 3.1 is known in advanced or at least the predictions are accessible in a black box setting. The functions $f(\cdot)$ and $h(\cdot)$ are also known in advance. In Table 1, several common monitoring statistics and physical constraints are introduced as guiding examples for the choice of $f(\cdot)$ and $h(\cdot)$.

If the monitoring scheme or physical constraints are not known, the functions can be chosen as the identity and variance function by default as introduced in the steel rolling case study in Section 4.2.

TABLE 1
EXAMPLES FOR THE CHOICE OF $f(\cdot)$ AND $h(\cdot)$

Monitoring Scheme	$f(\cdot)$	Physical Constraint	$h(\cdot)$
X-bar & S Charts By default	Identity + Variance	Smooth changes over time	$u_{ij,t}^A - u_{ij,t-1}^A$
Hottelling Control Chart	T^2 statistic	Sparse changes over time	$\ u_{ij,t}^A - u_{ij,t-1}^A\ _1$
Kernel Methods (e.g., SVM or PCA)	Corresponding Kernel function	Limited variation patterns	$\ u_{ij,t}^A - u_{ij,t-1}^A\ _*$
Gradient Boosting	Weighted sum of weak learners	Piecewise constant changes	Fused lasso penalty [31]
Neural Network Architectures	Inverse network function via back-propagation [32]	Variables within physically possible limits	$\ u_{ij,t}^A\ _2^2$ with appropriate Lagrange multiplier λ_2

$\|\cdot\|_*$ denotes the nuclear norm.

3.3 Solution Procedure

The SAGE problem formulation is an inherently nonconvex and NP-hard problem. If only the first two terms are considered, and the functions $g_{ij,k}$ and f are affine functions and the problem can be solved efficiently [33]. This is a result from the field of difference of convex (DC) programming, where problems have the form.

$$\min -g(x) + f(x) \quad (3)$$

where $x \in \mathbb{R}^n$ is the optimization variable and the functions $g: \mathbb{R}^n \rightarrow \mathbb{R}$ and $f: \mathbb{R}^n \rightarrow \mathbb{R}$ are convex. Algorithms such as branch and bound can solve DC problems to global optimality but requires a high computation effort [34-36]. However, all terms of the SAGE framework are necessary in the majority of applications, and the monitoring statistics is nonconvex. If a closed form expression is available, nonconvex solvers such as the Branch-And-Reduce Optimization Navigator (BARON) can be utilized to solve the non-convex formulation to global optimum [37]. However, no in-depth optimization knowledge is required for SAGE attacks, since this problem can be solved efficiently using heuristic methods like the genetic algorithm (GA) or stochastic gradient descent (SGD).

In the remainder of the paper, GA is used to solve the SAGE problem. When using GA with common software platforms, a few best practices should be considered. While the GA is commonly initialized with a random selection of design space points, the attacks should be initialized with historic, in-control data. This will lead to much faster convergence. Furthermore, choosing upper and lower bounds within physical limits of the data (e.g., image pixel values from 0 to 255, system variables within 6σ limits) will reduce the probability of detection and drastically reduce the solution space of the problem. Each phase in a GA run involves the selection of multiple parameters, however common software implementations are usually robust to the values chosen for these parameters [38].

In general, the choice of tuning parameters of the SAGE formulation is crucial to the efficacy of the attack. Therefore, binary search was adapted to find the optimal set of tuning parameters.

Binary Search for Hyperparameter tuning of SAGE formulation

(1) **Input:**

Parameters $Y_{k,t}^{ref}$, B_{k0} , $g_{ij,t}$, u_t^A , u_t^C
 Attack Effectivity (AE) Thresholds α_1
 Average Perturbation (AP) Threshold α_2
 Attack Cost (AC) Threshold α_3
 Maximum iterations max_{iter}

(2) **Initialize:** $\lambda_{l,min} = 0$, $\lambda_{l,max} = 1$, $\lambda_l = \lambda_{l,min}$, $l = 1, 2, 3$
 Counter $C=0$

(3) **Repeat SAGE attack**

(5) If $AE < \alpha_1$

$\lambda_{1,max} = \lambda_1$, $\lambda_{2,max} = \lambda_2$
 $\lambda_1 = (\lambda_{1,min} + \lambda_{1,max})/2$, $\lambda_2 = (\lambda_{2,min} + \lambda_{2,max})/2$
 $C=C+1$

(6) If $AP > \alpha_2$

$\lambda_{1,min} = \lambda_1$, $\lambda_{2,min} = \lambda_2$
 $\lambda_1 = (\lambda_{1,min} + \lambda_{1,max})/2$, $\lambda_2 = (\lambda_{2,min} + \lambda_{2,max})/2$

$C=C+1$
 (7) If $AC > \alpha_3$
 $\lambda_{3,min} = \lambda_3$
 $\lambda_3 = (\lambda_{3,min} + \lambda_{3,max})/2$
 $C=C+1$
 (8) If $C > max_{iter}$
 Break
 (8) Else if
 Break
 (12) End
 (13) End

The binary search considers the three main objectives of the attacker and tunes the hyperparameters λ_l , $l = 1, 2, 3$ until the Attack Effectivity (AE), Average Perturbation (AP) and the Attack Cost (AC) are within prescribed limits. The Attack Effectivity can either be computed by the first SAGE term or by an attack specific metric considering the attacked system model. Similarly, the Average Perturbation can be derived from the second and third SAGE terms or from the defenders monitoring algorithm. The Attack Cost is directly calculated from the fourth SAGE term.

4 CASE STUDIES

In this section, we use two case studies to validate the SAGE methodology proposed in Section 3. We will demonstrate how to use the proposed framework for image data as well as for functional curves.

4.1 Case Studies with Image Data

The goal of this simulation study is to illustrate how the potential of the SAGE framework to deceive state-of-the-art methods for image anomaly detection. This provides a generalization to the previous research in the field of adversarial examples for machine learning. Furthermore, we provide a case for the severe consequences of small but intentional perturbations to control variables on image responses in CPS. Therefore, we will attack both the smooth sparse decomposition (SSD) method [9], which is a benchmark image denoising and anomaly detection algorithm in the field of manufacturing, and a CNN-LIME, which is a state-of-the-art method in the field of classification and object detection.

The dataset used for both attacks is the Northeastern University (NEU) surface defect database [39], [40], [41], which contains six typical surface defects of hot-rolled steel strips. The dataset includes 1,800 grayscale images, with 300 samples of each of the six different surface defects (i.e., rolled-in scale (RS), patches (Pa), crazing (Cr), pitted surface (PS), inclusion (In) and scratches (Sc)).

4.1.1. SAGE Attack on SSD Method

Firstly, we attack the SSD method [9], which decomposes an image into three components: A smooth image background, the sparse anomalous regions, and the random noises, as illustrated in Fig. 2.

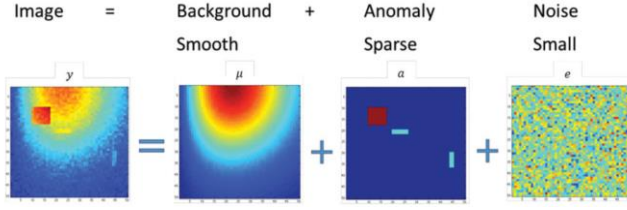


Fig. 2. Decomposition of image into background, anomaly, and noise [9]

The goal of the attack is to add small perturbations to the image, which are indistinguishable from the original image for the human eye and cannot be detected by designated detection algorithms. However, they will lead to a bad system response. In this case, the system response is the anomaly region, and we want to change the anomaly region as much as possible. When decomposing the image into background, anomaly, and noise via SSD, we want to detect the anomalies in different regions than where they actually are. This means, when the operators try to fix the problem, they will draw a wrong conclusion regarding the root cause of the anomalies and make the damage even worse by taking the wrong actions. In this circumstance, the SAGE attack formulation reduces to the following optimization problem.

$$\min_{y_t^A} - \|\theta_\alpha - \theta_\alpha^{SSD}(y_t^A)\|_F^2 + \lambda_1 \|y_t^{original} - y_t^A\|_F^2 + \lambda_3 C(y_t^A) \quad (4)$$

where y_t^A denotes the image that the attacker will inject into the system at time t , θ_α denotes the fixed and known anomaly region, θ_α^{SSD} is a function of y_t^A and denotes the extracted anomaly region from the attacker's image. The goal of the attacker is to maximize the damage by letting θ_α^{SSD} be as far away as possible from the ground truth anomaly θ_α . Furthermore, to not get detected the attackers' image should be close to the original image before the attack $y_t^{original}$. Since the monitoring of a process usually consists of streaming data from each time step t , the added perturbations in consecutive time steps should not be too different since this might be physically impossible. Furthermore, extreme changes over time might alert appropriate detection algorithms and lead to detection. This behavior is enforced by the third term in the formulation. The difference of the first three terms is calculated in terms of the squared Frobenius norm. Additionally, since the cost increases with the number of pixels attacked in an image, the cost function is chosen as the l_1 -norm to induce sparsity and attack as few pixels as possible.

As shown in Fig. 3, the image before and after the attack are almost indistinguishable to the human eye.

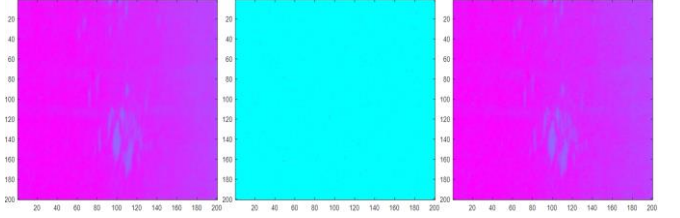


Fig. 3. Original image (left), added perturbations (middle) and attacked image (right) of steel surface defect

On the other hand, the outputs of the SSD algorithm before and after the attack are quite different (Fig. 4). After the attack, the false alarm rate has increased significantly since many regions are now identified incorrectly as surface defects.



Fig. 4. Recovered anomaly using SSD from the original image (left), anomaly from the attacked image (middle) and difference between anomaly region of original and attack image in red (left)

To show the generality of the SAGE formulation in attacking multiple classes of anomalies, 4 images are selected randomly from 5 anomaly classes and the following metrics are defined corresponding to the objectives of the attacker.

- Attack effectivity $AE = \frac{\sum_{i>0} (\|\theta_\alpha^{original} - \theta_\alpha^A\|)}{\sum_{i>0} (\theta_\alpha^A)}$
- Average Pixel Perturbation $APP = \frac{\sum_{k=1}^n \sum_{l=1}^m |Y_{kl}^{original} - Y_{kl}^A|}{n \cdot m \cdot 255}$

where n and m denote the height and width of the image, respectively. In this case study the images have the size $n=m=200$. The larger the attack effectivity, the more damage the attacker can do to the anomaly region; and the smaller the average pixel perturbation, the closer the attacked image will be to the original image. Note that the APP is scaled by 255 to account for the range of the pixel intensity values from 0 to 255. The results of those metrics for the 20 images are shown in Fig. 5.

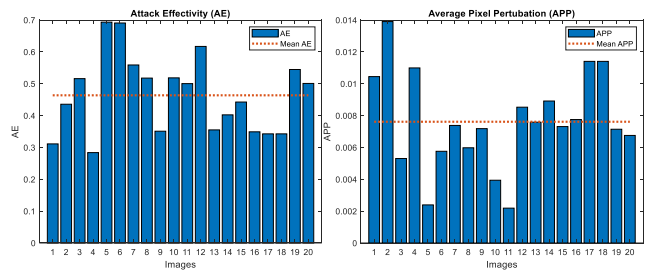


Fig. 5. Attack effectivity (left) and Average pixel perturbation (right) for 20 images

The average of the attack effectivity is 0.4637, so almost half of the anomalies can be changed, while the mean of the average pixel perturbation is only 0.0076.

The convergence of the genetic algorithm in this case study is quite fast and reaches a stable optimum after approximately 20 generations. While there is no guarantee in terms of global optimum, this is not the main focus of an attacker. An attacker only needs to achieve one bad system response to make damage, while in other circumstances the global optimality is much more desirable for example to achieve controllability and diagnosability.

As we can see from the results of the surface defects, after applying small but intentional perturbations via the SAGE framework, the SSD algorithm can be fooled by falsely detecting anomaly regions, while generating an attack image that is virtually indistinguishable for the human eye. This case study shows the generality of the SAGE framework when applied to image data even for complex anomaly detection algorithms like SSD, which utilize advanced optimization techniques. Therefore, our proposed framework can easily be adapted for other image anomaly detection methods as long as the detection algorithms parameters are explicitly known or at least predictions from the detection algorithm can be accessed in a black box manner.

4.1.2. SAGE Attack on CNN-LIME

Furthermore, a Convolutional Neural Network in combination with Local Interpretable Model-Agnostic Explanations (CNN-LIME) [42] is attacked. LIME explains the prediction of any classifier by treating it as a black box model, by learning an interpretable model locally around the prediction. LIME finds the region of an image that led to the classification of that image to a particular class. In view of this fact, it is related to object detection algorithms that locate objects of interest in an image by predicting a boundary around the object. Based on previous research [43], [25], [44], [45], object detection algorithms are much more difficult to attack [45]. Therefore, attacking CNN-LIME will demonstrate the immense capabilities of the proposed SAGE formulation in attacking a wide range of algorithms.

To obtain a good classification model, transfer learning with weights from the MobileNet is utilized. An 99.9% model accuracy can be achieved by initializing the CNN architecture with those weights and fine tuning it on the NEU surface detection dataset. The corresponding confusion matrix is visualized in Fig. 6.

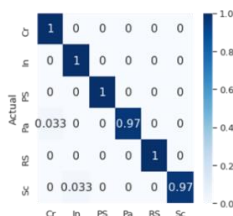


Fig. 6. Confusion Matrix of CNN Model

Afterwards the LIME algorithm is utilized to explain the predictions of the CNN model and identify the anomaly regions in the images.

The SAGE formulation is adopted as follows in this setting.

$$\begin{aligned} \min_{y_t^A} & -\|\theta_t^{original} - \theta^{CNN}(y_t^A)\|_F^2 \\ & -\lambda_0 \|\xi^{original} - \xi^{LIME}(y_t^A)\|_F^2 \\ & +\lambda_{1,1} \|y_t^{original} - y_t^A\|_F^2 \\ & +\lambda_{1,2} \|\text{vec}(y_i^{original} - y_i^A) \cdot \mathcal{D} \cdot \text{vec}(y_i^{original} - y_i^A)\|_F^2 \\ & +\lambda_3 \mathcal{C}(y_i^A) \end{aligned} \quad (5)$$

where θ denotes the predicted class probabilities and ξ is the explanation produced by LIME for the class predictions. The intuition of this attack is to misclassify the anomaly images, while keeping the attacker's image close to the original image and changing the explanatory region away from the original one to make the attackers malicious class prediction seem legitimate. Furthermore, the changes in the image should be smooth to preserve the spatial dependencies to avoid detection. Therefore, the smoothness penalty $\lambda_{1,2} \|\text{vec}(y_t^{original} - y_t^A) \cdot \mathcal{D} \cdot \text{vec}(y_t^{original} - y_t^A)\|_F^2$ is applied, where

$$\mathcal{D} = \begin{bmatrix} 1 & -1 & & & \\ -1 & 2 & -1 & & \\ & \ddots & \ddots & \ddots & \\ & & -1 & 2 & -1 \\ & & & -1 & 1 \end{bmatrix}$$

is the second-order smoother that applies to the vectorized difference between the original and the attacker's image.

Similar to the image attack on the SSD algorithm, the attacker's image can hardly be distinguished from the original one as shown in Fig. 7.

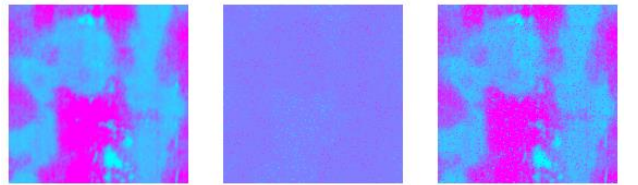


Fig. 7. Original image (left), added perturbations (middle) and attacked image (right) of surface defect

On the other hand, the classification result changes significantly as summarized in Table 2.

TABLE 2
CLASSIFICATION RESULTS BEFORE AND AFTER ATTACK

Class Label	RS	PS	Cr	Pa	In	Sc
Before Attack	0.001	0.000	0.002	0.996	0.001	0.001
After Attack	0.001	0.012	0.179	0.195	0.514	0.099

The highest class probability in **bold**.

In this attack formulation, the goal was to misclassify a

given true process anomaly class as any of the remaining five class labels. From Table 2, we can see that the correct class patches (Pa) was identified with very high confidence (99.6%) before the attack. After the attack, the probability of the correct class reduces to 19.5% and the class inclusion (In) was chosen with highest confidence (51.4%). Any other process anomaly class can be attacked in a similar fashion as illustrated in this case study with the process anomaly patches (Pa). If the attacker not only wants to misclassify the anomalies but also assigns the picture to a specific prescribed class, the first penalty term in Equation (4) can be adjusted accordingly. The goal of the attack was also to change the explanatory region derived via LIME as far as possible from the original one to avoid any suspicion and justify the differently classified anomaly after the SAGE attack on the image. Fig. 8 shows this severe change in explanatory region after the attack.



Fig. 8. Original explanatory region computed via LIME (left), change in explanatory region (middle) and attacked explanatory region (right) of surface defect

The small pixels around the identified regions after the attack coincide with the inclusion anomaly, which has the highest-class probability after the attack. This will avoid detection by the defender while leading to wrong conclusions about the underlying process anomaly.

In summary, the SSD algorithm is much more vulnerable to perturbations than CNN-LIME. The SSD attacks exploits very few weak spots in the image and changes the pixel value significantly to destroy the smoothness of the background. The CNN-LIME attack has a slightly higher APP of 0.032. To change the classification result to a different class of only six possible ones, a much large number of pixels needs to be attacked. Therefore, the CNN attack is a much more challenging task. However, the SAGE formulation can exploit the weaknesses of both SSD and CNN-LIME very effectively, while not utilizing any knowledge about the specific parameters and weaknesses of the two respective algorithms. In view of this fact, the SAGE attack provides an effective generalization for existing adversarial example generation schemes in the setting of a black-box attacks.

4.2 Case Studies with Functional Curve Data

To show the vulnerability of common CPS to stealthy attacks, a MATLAB Simulink testbed [46] for one stage plate rolling is used to show the devastating effect of small but worst-case perturbations to functional curves in CPS. The testbed uses a Multiple Input Multiple Output (MIMO)

LQG regulator to control the horizontal and vertical thickness of a steel beam in a hot steel rolling mill.

In this case study, the SAGE formulation reduces to the following optimization problem.

$$\min_{u_t^A} -\|Y_t^{ref} - B_0 - \sum_{j=1}^4 \beta_j u_{ij}^A\|_2^2 + \lambda_1 \|u_t^{IC} - u_t^A\|_2^2 + \lambda_2 \|u_t^A - u_{t-1}^A\| + \lambda_3 C(u_t^A) \quad (6)$$

where Y_t^{ref} denotes the engineering specification of quality response and is constant in this case. Since the system response in this case is measured in terms of x- and y-axis thickness variation, the goal would be to have no variation so $Y_t^{ref} = 0$. In this case u_t^{IC} is chosen as historic data of the same length as the attack to mimic a replay attack. Furthermore, the tuning parameters are chosen via binary search as follows:

- $\lambda_1 = 15.5$
- $\lambda_2 = 5$
- $C(u_{ij,t}^A) = \begin{cases} 0, & \text{for } j = 1, 3 \\ 2, & \text{for } j = 2, 4 \end{cases}$

The cost function represents the fact that the roll gap ($j = 1, 3$) is easy to attack while the roller force ($j = 2, 4$) requires more efforts.

The optimization problem was solved using GA and tuned via binary search to achieve the three objectives of the attacker. For better visualization, only the first 100 time steps of the attack are visualized in the following figures. The attack clearly avoids detection by the x bar chart as visualized in Fig. 9.

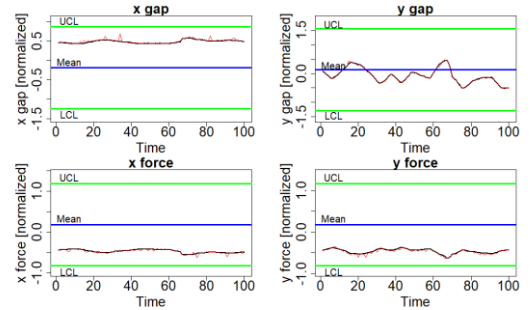


Fig. 9. Attackers' control actions (red) and in control data (black) within 3σ limits

On the other hand, the attack leads to maximal damage on the system response, which is far outside of the 3 sigma limits of the control chart (Fig. 10)

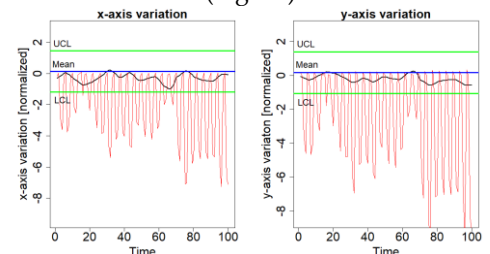


Fig. 10. Attackers' control actions (red) far outside of 3σ limits

However, when looking at the difference of the correlation matrices in control and attack data (Table 3), we can see that the correlation structure is still different, which could lead to detection by the anomaly detection methods. The difference in correlation structure was calculated as the average of absolute difference of attack and in control correlation matrix in a 100 time step sliding window over the entire dataset.

TABLE 3
ABSOLUTE DIFFERENCE BETWEEN IN CONTROL AND ATTACK
CORRELATION MATRIX

	x gap	x force	y gap	y force
x gap	0			
x force	0.305	0		
y gap	0.038	0.014	0	
y force	0.161	0.109	0.017	0

Therefore, the first penalty term of the SAGE formulation is extended to incorporate a similarity in terms of correlation structure as well.

$$\begin{aligned}
& \min_{\mathbf{u}_t^A} -\|Y_t^{ref} - B_0 - \sum_{j=1}^4 \beta_j u_{t,j}^A\|_2^2 + \lambda_{1,1} \|\mathbf{u}_t^{IC} - \mathbf{u}_t^A\|_2^2 \\
& + \lambda_{1,2} \left\| \left\| \frac{\sum_{m=t-n}^t (\mathbf{u}_m^{IC} - \bar{\mathbf{u}}^{IC})^2}{n-1} - \frac{\sum_{m=t-n}^t (\mathbf{u}_m^A - \bar{\mathbf{u}}^A)^2}{n-1} \right\|_2 \right\|_2^2 \\
& + \lambda_2 \|\mathbf{u}_t^A - \mathbf{u}_{t-1}^A\|_2^2 + \lambda_3 C(\mathbf{u}_t^A) \quad (7)
\end{aligned}$$

where $\bar{\mathbf{u}}^{IC}$ and $\bar{\mathbf{u}}^A$ denote the process mean of the in-control data and attack data, respectively. The new set of tuning parameters is chosen as follows.

- $\lambda_{1,1} = 15.5$ to escape mean monitoring
- $\lambda_{1,2} = 12$ to escape variance monitoring
- $\lambda_2 = 5$ physical constraint
- $\lambda_3 = 1$ cost function

Furthermore, a sliding window of $n = 100$ is used to compute the standard deviation in the added penalty term. To compute the initial sliding window, the first 100 time steps of the new attack are initialized with previous results. To ensure the correlation structure was fully considered afterwards, the first 200 time steps are discarded and not used by the attacker. As we can see from Fig. 11, that the signal of the in control (black) and attack (red) are almost completely aligned. Therefore, they are indistinguishable for a human operator and hard to be detected by a control chart or other anomaly detection methods.

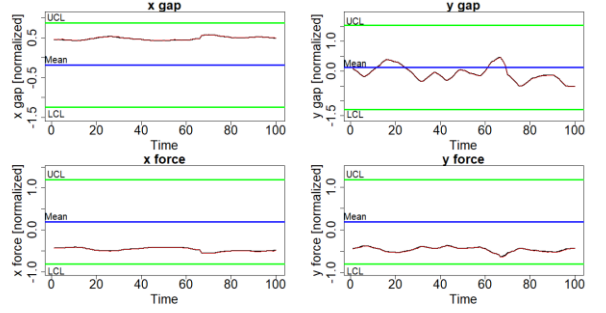


Fig. 11. Attackers' control actions (red) and in control data (black) within 3σ limits

On the other hand, the SAGE attack can still cause a very abnormal system response (Fig. 12), which fulfills the main objectives of an attacker.

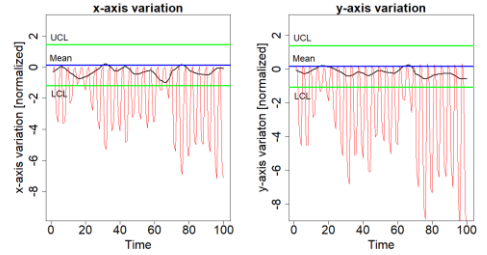


Fig. 12. Attackers' control actions (red) far outside of 3σ limits

After including a corresponding term into the SAGE formulation, the correlation structure of in control and attack data shows no significant difference (Table 4).

TABLE 4
ABSOLUTE DIFFERENCE BETWEEN IN CONTROL AND ATTACK
CORRELATION MATRIX

	x gap	x force	y gap	y force
x gap	0			
x force	0.007	0		
y gap	0.014	0.016	0	
y force	0.009	0.002	0.023	0

To show that small perturbations of the control variables can lead to a large change of the system response, the Attack Effectivity (AE) and Average Perturbation (AP) are computed as follows.

- Attack effectivity $AE = \frac{\sum_{t=1}^n (\sum_{j=1}^4 \|u_{t,j}^{IC} - u_{t,j}^A\|/n)}{(\sum_{j=1}^4 \sigma_{u_j^{IC}})}$
- Average Perturbation $AP = \frac{\sum_{t=1}^n \|Y_t^{ref} - Y_t^A\|/n}{\sigma_Y}$

where n denotes the length of the attack, $\sigma_{u_j^{IC}}$ the in-control standard deviation of control variable j , σ_Y the in-control standard deviation of the system responses and Y_t^A is the resulting system response of the attack. Those metrics essentially measure the absolute distance of in-control and attack in terms of the number of in-control standard

deviations. The results are summarized in Table 5 and show the significant decrease of perturbation from 0.129 (Attack 1, Eq. 6) to 0.037 (Attack 2, Eq. 7), while keeping the damage measured in terms of AE at a similar level.

TABLE 5
ATTACK EFFECTIVITY AND AVERAGE PERTUBATION OF THE TWO SAGE ATTACK FORMULATIONS

	AE	AP
Attack 1 (Eq. 6)	10.796	0.129
Attack 2 (Eq. 7)	10.636	0.037

To further evaluate the effectivity of the two proposed SAGE attacks, seven machine learning techniques commonly used by previous research for cyber-attack detection algorithms in CPS are evaluated for their effectiveness to detect stealthy attacks (Table 6). The hyperparameters of the respective methods were tuned via grid search, to achieve the best detection results possible. In particular, a Support Vector Machine (SVM), k Nearest Neighbor (kNN), Random Forest (RF), Bagging, Gradient Boosting Machine (GBM), Decision Tree (DT), and a Deep Neural Network (DNN) were used to classify the presence of an attack.

TABLE 6
ACCURACY (ACC.), PRECISION (PREC.), AND RECALL (REC.) AND F1-SCORE OF DIFFERENT MACHINE LEARNING METHODS

Method	Attack 1: SAGE formulation (Eq. 6)				Attack 2: SAGE formulation considering correlation structure (Eq. 7)			
	Acc.	Prec.	Rec.	F1	Acc.	Prec.	Rec.	F1
SVM	0.671	0.797	0.674	0.635	0.623	0.784	0.625	0.563
kNN	0.458	0.445	0.460	0.419	0.394	0.394	0.394	0.394
RF	0.554	0.568	0.555	0.533	0.497	0.497	0.497	0.495
Bagging	0.545	0.547	0.546	0.542	0.420	0.420	0.420	0.420
GBM	0.574	0.575	0.575	0.573	0.497	0.748	0.501	0.334
DT	0.520	0.625	0.524	0.401	0.497	0.748	0.501	0.334
DNN	0.946	0.952	0.947	0.946	0.496	0.248	0.500	0.332

The results in Table 6 show, that the DNN can detect the attacks generated by the first SAGE attack (Eq. 6) with very high accuracy (94.6%). In contrast to the other six methods, the DNN can capture a significant difference in the correlation structure as investigated in Table 3. The high precision, recall, and F1-score of the DNN confirm these results. The other methods cannot capture the difference in the correlation structure and do not exhibit sufficient detection performance.

However, if the SAGE formulation (Attack 2) is adjusted to consider the correlation structure of the variables (Eq. 7), none of those six methods can achieve satisfactory detection performance. While the SVM performs the best, its detection accuracy of 62.3% is not sufficient for reliable and fast attack detection. This example shows how flexible the SAGE formulation can be adjusted to make the existing detection algorithms not effective.

Even in the case of black-box attacks, where the detection algorithm is not known to the attacker, the proposed

SAGE framework can cause severe damage to a system while staying undetected by commonly used machine learning classifiers. This provides a strong case for the generality and effectivity of the proposed framework, which can not only exploit weaknesses of particular algorithms through its flexible formulation, but also make replay non-essential for effective attacks by mimicking the normal operating conditions.

5 CONCLUSION

We have introduced a holistic framework for attack generation in CPS (SAGE), which incorporates the three main objectives of an attacker (maximize damage, avoid detection, minimize the attack cost) and the physical constraints of the CPS. By solving the proposed optimization problem, SAGE can generate stealthy worst-case perturbations that fulfill all the objectives of the insider attacker. This framework provides a general formulation to target any algorithm used for cyber-attack detection in CPS as long as the formulation is known to the attacker. Even if no specific knowledge of the detection method is available (black-box attack), state-of-the-art machine learning techniques can be fooled by mimicking the normal operating conditions as verified in the case studies.

This research contributes to the understanding of stealthy attacks in CPS. As our research shows, properly executed insider attacks, that mimic the same generative process as normal, in-control data, cannot be handled by many existing anomaly detection methods. This implies that future detection algorithms should not rely on readily available anomaly detection techniques but study the stealthy and adversarial behavior of cyber-attacks.

The proposed method can be accessed in the supplementary material of this paper with examples in three popular software languages (Python, R, MATLAB) and provides a new benchmark for researchers and practitioners for the design of more efficient detection algorithms and more robust and resilient CPS design.

ACKNOWLEDGMENT

This research is funded by the National Science Foundation Award ID 2019378.

REFERENCES

- [1] A.E. Elhabashy, L.J. Wells, and J.A. Camelio, Cyber-Physical Security Research Efforts in Manufacturing—A Literature Review. *Procedia Manufacturing*, 2019. 34: p. 921-931.
- [2] D. Ding, Q.-L. Han, Y. Xiang, X. Ge, and X.-M. Zhang, A survey on security control and attack detection for industrial cyber-physical systems. *Neurocomputing*, 2018. 275: p. 1674-1683.
- [3] Ponemon Institute, Cost of Insider Threats Global Report. 2020.
- [4] J. Minnick, "The Biggest Cybersecurity problems facing manufacturing in 2016," *Manufacturing Business Technology*, 2016.
- [5] F. Li, Q. Li, J. Zhang, J. Kou, J. Ye, W. Song, and H.A. Mantooth, "Detection and Diagnosis of Data Integrity Attacks in Solar Farms Based on Multilayer Long Short-Term Memory Network,"

- IEEE Transactions on Power Electronics*, 2020. 36(3): p. 2495-2498.
- [6] Q. Li, F. Li, J. Zhang, J. Ye, W. Song, and A. Mantooth, "Data-driven Cyberattack Detection for Photovoltaic (PV) Systems through Analyzing Micro-PMU Data," *IEEE Energy Conversion Congress and Exposition (ECCE)*, 2020.
 - [7] M. Wu, and Y.B. Moon, "Intrusion detection system for cyber-manufacturing system," *Journal of Manufacturing Science and Engineering*, 2019. 141(3).
 - [8] F. Zhang, H.A.D.E. Kodituwakku, J.W. Hines, and J. Coble, "Multilayer data-driven cyber-attack detection system for industrial control systems based on network, system, and process data," *IEEE Transactions on Industrial Informatics*, 2019. 15(7): p. 4362-4369.
 - [9] H. Yan, K. Paynabar, and J. Shi, "Anomaly detection in images with smooth background via smooth-sparse decomposition," *Technometrics*, 2017. 59(1): p. 102-114.
 - [10] B.C. Ervural, and B. Ervural, "Overview of cyber security in the industry 4.0 era," *Industry 4.0: managing the digital transformation*. 2018, Springer. p. 267-284.
 - [11] F. Li, A. Shinde, Y. Shi, J. Ye, X.-Y. Li, and W. Song, "System statistics learning-based IoT security: Feasibility and suitability," *IEEE Internet of Things Journal*, 2019. 6(4): p. 6396-6403.
 - [12] F. Li, Y. Shi, A. Shinde, J. Ye, and W. Song, "Enhanced cyber-physical security in internet of things through energy auditing," *IEEE Internet of Things Journal*, 2019. 6(3): p. 5224-5231.
 - [13] Homeland Security Centre for the Protection of National Infrastructure, "Cyber security assessments of industrial control systems", available at <https://www.ccn-cert.cni.es/publico/InfraestructurasCriticaspublico/CPNI-Guia-SCI.pdf>, 2011
 - [14] S. Han, M. Xie, H.-H. Chen, and Y. Ling, "Intrusion detection in cyber-physical systems: Techniques and challenges," *IEEE Systems Journal*, 2014. 8(4): p. 1052-1062.
 - [15] Y. Guan, and X. Ge, "Distributed attack detection and secure estimation of networked cyber-physical systems against false data injection attacks and jamming attacks," *IEEE Transactions on Signal and Information Processing over Networks*, 2017. 4(1): p. 48-59.
 - [16] F. Pasqualetti, F. Dörfler, and F. Bullo, "Attack detection and identification in cyber-physical systems", *IEEE Transactions on Automatic Control*, 2013. 58(11): p. 2715-2729.
 - [17] M. Feng, and H. Xu, "Deep reinforcement learning based optimal defense for cyber-physical system in presence of unknown cyber-attack," *IEEE Symposium Series on Computational Intelligence (SSCI)*. 2017.
 - [18] F. Li, R. Xie, B. Yang, L. Guo, P. Ma, J. Shi, J. Ye, and W. Song, "Detection and identification of cyber and physical attacks on distribution power grids with pvs: An online high-dimensional data-driven approach," *IEEE Journal of Emerging and Selected Topics in Power Electronics*, 2019.
 - [19] B. Yang, L. Guo, F. Li, J. Ye, and W. Song, "Vulnerability assessments of electric drive systems due to sensor data integrity attacks," *IEEE Transactions on Industrial Informatics*, 2019. 16(5): p. 3301-3310.
 - [20] M. Wu, Z. Song, and Y.B. Moon, "Detecting cyber-physical attacks in CyberManufacturing systems with machine learning methods," *Journal of intelligent manufacturing*, 2019. 30(3): p. 1111-1123.
 - [21] Y. Mo, and B. Sinopoli, "Integrity attacks on cyber-physical systems," *Proceedings of the 1st International Conference on High Confidence Networked Systems*. 2012.
 - [22] J. Li., J.Y. Lee, Y. Yang, J.S. Sun, and K. Tomsovic, "Conaml: Constrained adversarial machine learning for cyber-physical systems," 2020, *arXiv preprint arXiv:2003.05631*
 - [23] M. Sharif, S. Bhagavatula, L. Bauer, and M.K. Reiter, A general framework for adversarial examples with objectives. *ACM Transactions on Privacy and Security (TOPS)*, 2019. 22(3): p. 1-30.
 - [24] K. Eykholt., I. Evtimov, E. Fernandes, B. Li, A. Rahmati, C. Xiao, A. Prakash, T. Kohno, and D. Song, "Robust physical-world attacks on deep learning visual classification," *Proceedings of the IEEE Conference on Computer Vision and Pattern Recognition*. 2018.
 - [25] A. Kurakin, I. Goodfellow, and S. Bengio, "Adversarial examples in the physical world," *ICLR Workshop*, 2017
 - [26] I.J. Goodfellow., J. Shlens, and C. Szegedy, "Explaining and harnessing adversarial examples," *International Conference on Learning Representations*, 2015
 - [27] J. Kos, I. Fischer, and D. Song, "Adversarial examples for generative models," *IEEE Security and Privacy Workshops*, 2018
 - [28] M. Aladag, F.O. Catak, and E. Gul, "Preventing data poisoning attacks by using generative models," *1st International Informatics and Software Engineering Conference (UBMYK)*, 2019
 - [29] D. Wang, C. Li, S. Wen, S. Nepal, and Y. Xiang, "Man-in-the-Middle Attacks against Machine Learning Classifiers via Malicious Generative Models," *IEEE Transactions on Dependable and Secure Computing*, 2020.
 - [30] B. Chen, C. Schmittner, Z. Ma, W.G. Temple, X. Dong, D.L. Jones, and W.H. Sanders, "Security analysis of urban railway systems: the need for a cyber-physical perspective," *International Conference on Computer Safety, Reliability, and Security*. 2014. Springer.
 - [31] R. Tibshirani, M. Saunders, S. Rosset, J. Zhu, and K. Knight, "Sparsity and smoothness via the fused lasso," *Journal of the Royal Statistical Society: Series B (Statistical Methodology)*, 2005. 67(1): p. 91-108.
 - [32] C.A. Jensen, R.D. Reed, R.J. Marks, M.A. El-Sharkawi, J.-B. Jung, R.T. Miyamoto, G.M. Anderson, and C.J. Eggen, "Inversion of feedforward neural networks: Algorithms and applications," *Proceedings of the IEEE*, 1999. 87(9): p. 1536-1549.
 - [33] S. Boyd, and L. Vandenberghe, "Convex optimization," *Cambridge university press*, 2004.
 - [34] E.L. Lawler, and D.E. Wood, "Branch-and-bound methods: A survey," *Operations Research*, 1966. 14(4): p. 699-719.
 - [35] N. Agin, "Optimum seeking with branch and bound," *Management Science*, 1966. 13(4): p. B-176-B-185.
 - [36] X. Shen, S. Diamond, Y. Gu, and S. Boyd. "Disciplined convex-concave programming," *2016 IEEE 55th Conference on Decision and Control (CDC)*, 2016.
 - [37] J. Liu, N. Ploskas, and N.V. Sahinidis, "Tuning BARON using derivative-free optimization algorithms," *Journal of Global Optimization*, 2019. 74(4): p. 611-637.
 - [38] F. Ortiz Jr, J.R. Simpson, J.J. Pignatiello Jr, and A. Heredia-Langner, "A genetic algorithm approach to multiple-response optimization," *Journal of Quality Technology*, 2004. 36(4): p. 432-450.
 - [39] H. Dong, K. Song, Y. He, J. Xu, Y. Yan, and Q. Meng, PGA-Net: Pyramid feature fusion and global context attention network for automated surface defect detection. *IEEE Transactions on*

- Industrial Informatics*, 2019. 16(12): p. 7448-7458.
- [40] Y. He, K. Song, Q. Meng, and Y. Yan, "An end-to-end steel-surface defect detection approach via fusing multiple hierarchical features," *IEEE Transactions on Instrumentation and Measurement*, 2019. 69(4): p. 1493-1504.
 - [41] K. Song, and Y. Yan, "A noise robust method based on completed local binary patterns for hot-rolled steel strip surface defects," *Applied Surface Science*, 2013. 285: p. 858-864.
 - [42] M.T. Ribeiro, S. Singh, and C. Guestrin. "Why should i trust you? Explaining the predictions of any classifier," *Proceedings of the 22nd ACM SIGKDD international conference on knowledge discovery and data mining*. 2016.
 - [43] J.H. Metzen, M. Chaithanya Kumar, T. Brox, and V. Fischer. "Universal adversarial perturbations against semantic image segmentation," *Proceedings of the IEEE International Conference on Computer Vision*. 2017.
 - [44] V. Fischer, M.C. Kumar, J.H. Metzen, and T. Brox, "Adversarial examples for semantic image segmentation," *ICCV*, 2017
 - [45] C. Xie, J. Wang, Z. Zhang, Y. Zhou, L. Xie, and A. Yuille. "Adversarial examples for semantic segmentation and object detection," *Proceedings of the IEEE International Conference on Computer Vision*. 2017.
 - [46] MATLAB Simulink : Beam Thickness Control. Available from: <https://www.mathworks.com/help/control/ug/thickness-control-for-a-steel-beam.html>.



Michael Biehler received his B.S. and M.S in Industrial Engineering and Management from Karlsruhe Institute of Technology (KIT) in 2017 and 2020, respectively. Currently, he is a Ph.D. student in the Stewart School of Industrial and Systems Engineering, Georgia Institute of Technology. His research rests at the interface between machine learning and cyber physical (manufacturing) systems, where he aims to develop methods for cyber security, monitoring, prognostics and control. He is a member of ASME, ENBIS, IEEE, IISE, INFORMS and SIAM.



Zhen Zhong received the B.S. degree in Electrical Engineering from University of Science and Technology of China, Anhui, China, in 2017. Currently, he is a Ph.D. student at the H. Milton Stewart School of Industrial and Systems Engineering, Georgia Institute of Technology. His research interests include the process control and high dimensional data analytics in semiconductor manufacturing.



Dr. Jianjun Shi received the B.S. and M.S. degrees in automation from the Beijing Institute of Technology in 1984 and 1987, respectively, and the Ph.D. degree in mechanical engineering from the University of Michigan in 1992.

Currently, Dr. Shi is the Carolyn J. Stewart Chair and Professor at the Stewart School of Industrial and Systems Engineering, Georgia Institute of Technology. His research interests include the fusion of advanced statistical and domain knowledge to

develop methodologies for modeling, monitoring, diagnosis, and control for complex manufacturing systems.

Dr. Shi is a Fellow of the Institute of Industrial and Systems Engineers (IISE), a Fellow of American Society of Mechanical Engineers (ASME), a Fellow of the Institute for Operations Research and the Management Sciences (INFORMS), an elected member of the International Statistics Institute (ISI), a life member of ASA, an Academician of the International Academy for Quality (IAQ), and a member of National Academy of Engineers (NAE).